Linking Single-Molecule Blinking to Chromophore Structure and Redox Potentials

Stein, Ingo H.; Capone, Stella; Smit, Jochem H.; Baumann, Fabian; Cordes, Thorben; Tinnefeld, Philip

Published in:
Chemphyschem

DOI:
10.1002/cphc.201100820

Publication date:
2012

DOI: 10.1002/cphc.201100820

Linking Single-Molecule Blinking to Chromophore Structure and Redox Potentials

Ingo H. Stein,[a, b] Stella Capone,[b] Jochem H. Smit,[c] Fabian Baumann,[b] Thorben Cordes,*[c] and Philip Tinnefeld*[a, b]

This paper is contributed in honor and admiration of Professor Christoph Bräuchle's outstanding scientific contributions

Intensity fluctuations between an ON-state and an OFF-state, also called blinking, are common to all luminescent objects when studied at the level of individuals. We studied blinking of three dyes from a homologous series (Cy3, Cy5, Cy7). The underlying radical anion states were induced by removing oxidants (i.e. oxygen) and by adding the reductant ascorbic acid. We find that for different conditions with distinct levels of oxidants in solution the OFF-state lifetime always increases in the order Cy3 < Cy5 < Cy7. Longer OFF-times are related to higher reduction potentials of the fluorophores, which increase with the size of the chromophore. Interestingly, we find reaction rates of the radical anion that are unexpectedly low at the assumed oxygen concentration. On the other hand, reaction rates meet the expectations of similar Rehm–Weller plots when methylviologen is used as oxidant, confirming the model of photoinduced reduction and oxidation reactions. The relation of OFF-state lifetimes to redox potentials might enable predictions about the nature of dark states, depending on the fluorophores' nano-environment in super-resolution microscopy.

1. Introduction

On the single-molecule level, essentially all fluorophores exhibit intensity fluctuations between an ON-state and an OFF-state that is referred to as blinking. Blinking is often caused by transitions into the triplet state or radical states.[1,2] Triplet states result from intersystem crossing and have a typical lifetime in the microsecond to lower millisecond range. Recently, it has been shown that radical ions formed as a result of one-electron transfer reactions can have a much longer lifetime of up to minutes (redox blinking).[3,4]

For a long time unpredictable blinking had been plaguing single-molecule experiments. Only in recent years, has blinking become more controllable and even valuable for optical super-resolution microscopy.[5–12] For microscopy techniques based on subsequent localization of single molecules, such as PALM, fPALM, STORM, GSDIM, dSTORM or Blink Microscopy, the majority of molecules has to be shelved to a transient dark state and the stochastically active molecules successively localized.[6–11] By repeating this procedure, all molecule positions are determined and super-resolved fluorescence images are reconstructed. For this method to work efficiently, the lifetimes of the dark states of the molecules have to be long enough so that a sufficient number of molecules can be co-localized within one diffraction-limited spot.[13] Presumed radical ion states have proven to be well-suited for super-resolution microscopy because they are generic dark states of all fluorophores.[10,13] On the other hand, single-molecule studies showed that the lifetimes of these dark states vary significantly between different dyes at otherwise identical conditions, indicating that some dyes are better suited for super-resolution microscopy than others.[10,11,14]

It has been argued that a higher reduction potential of the fluorophores, that is, a better-stabilized radical ion, should be accompanied by a longer OFF-state lifetime.[4] Accordingly, the reduction potential might be the parameter to evaluate dyes for localization-based super-resolution microscopy. This is why certain oxazine dyes with high reduction potentials have been chosen for super-resolution microscopy.[4] On the other hand, very recently, it has been shown that these oxazine dyes can undergo a second reduction, leading to a long-lived leuko form.[15] Then there is the general question about the nature of the underlying dark states in localization based super-resolution microscopy using the blinking of dyes.[10,11,16] To advance blinking-based super-resolution imaging, the understanding of the underlying dark states is crucial. In addition, the ability to predict the properties of dyes at the single-molecule level will foster further developments. A systematic study of chromo-

[a] I. H. Stein, Prof. Dr. P. Tinnefeld
NanoBioScience Group
Institute for Physical and Theoretical Chemistry
TU Braunschweig
Hans-Sommer-Str. 10, 38106 Braunschweig (Germany)
E-mail: p.tinnefeld@tu-braunschweig.de

[b] I. H. Stein, S. Capone, F. Baumann, Prof. Dr. P. Tinnefeld
Applied Physics-Biophysics & Center for NanoScience (CeNS)
Ludwig Maximilian University
Amalienstr. 54, 80799 München (Germany)

[c] J. H. Smit, Dr. T. Cordes
Molecular Microscopy Research Group & Single-molecule Biophysics
Zernike Institute for Advanced Materials
University of Groningen
Nijenborgh 4, 9747 AG Groningen (The Netherlands)
E-mail: t.m.cordes@rug.nl

phore properties and blinking is required to test the hypothesis of the correlation of blinking kinetics and reduction potentials.

Herein, we study the dependence of redox blinking on the electronic properties of dyes with a focus on the absorption wavelength and the reduction potential. To minimize other influences such as chromophore structure, for example due to chemical substituents, differing hydrophobicity or steric constraints, we used dyes from the homologous series of cyanine fluorophores. Cy3, Cy5, and Cy7 exhibit a systematic increase of their chromophore system and the energetic properties can be described well by the simple particle-in-the-box model (i.e. absorption wavelength and chromophore size are quantitatively connected by the number of delocalized π electrons, see Figure 1, $n = 1,2,3$). According to the Kuhn model,[17] the reduction potentials increase with the number of π electrons, that is, larger dyes within one series are reduced more easily than fluorophores with smaller conjugated π systems.

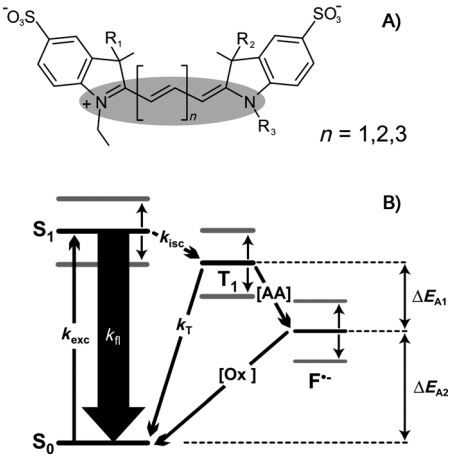

Figure 1. A) Overview of the chemical structures of the cyanine dyes used [$n = 1$ (Cy3), $n = 2$ (Cy5), $n = 3$ (Cy7)]. Residues are $R_1 = R_2 = CH_3$ and $R_3 = (C_5H_{10})$-CO_2NH-(C_6H_{12})-PO_4^--DNA for Cy3/Cy5; $R_1 = R_3 = (C_3H_6)$-SO_3^-, and $R_2 = (C_3H_6)$-CO_2-DNA for Cy7. The basic chromophore is highlighted in grey. B) Jablonski diagram of the fluorophores from one homologous series. One single molecule is excited from its singlet ground state S_0 into the first excited state S_1 by appropriate laser light with the excitation rate k_{exc}, fluorescence is observed with k_{fl}. Intersystem crossing occurs with the rate constant k_{isc} populating the triplet state T_1. The triplet has the intrinsic lifetime of $1/k_T$ but can also be depopulated by a photoinduced electron transfer originating from a reaction with ascorbic acid (AA). This reaction forms a radical anion (assuming a neutral fluorophore before the reaction) which is recovered to the electronic ground by an oxidation process mediated by molecular oxygen or MV. The energy levels of Cy5 are shown in black as a reference; Cy3 has blue-shifted absorption/emission while Cy7 shows a red-shifted absorption/emission. The energy of the triplet state and radical anion change accordingly.

We carried out single-molecule spectroscopy of cyanine dyes that were attached to DNA and immobilized with neutravidin/biotin on BSA-coated cover slips. We developed an assay to ensure comparable conditions in the experiments with different dyes, especially with respect to oxygen concentration. Redox blinking was induced by removing oxygen with the glucose oxidase/catalase (GOC) oxygen scavenging system and adding 75 μM of the reductant ascorbic acid (AA).[10] Single molecules were placed in the laser focus of a confocal microscope and fluorescence transients of redox blinking molecules were recorded. From these transients we extracted the OFF-state lifetime for the three cyanine derivatives. A strong correlation of chromophore size and OFF-state lifetime corroborates the idea that the simple model is able to predict qualitatively the OFF-state lifetime of cyanines, substantiating that the redox potentials are a crucial parameter for dye selection in super-resolution microscopy. In the future, deviations from such predictions might point towards a different nature of observed OFF-states.

2. Results and Discussion

We used three dyes from the homologous series of cyanine fluorophores, Cy3 ($\lambda_{max} = \sim 550$ nm), Cy5 ($\lambda_{max} = \sim 650$ nm), and Cy7 ($\lambda_{max} = \sim 750$ nm). These fluorophores are commonly used to label proteins and nucleic acids and also in demanding applications such as single-molecule FRET and super-resolution microscopy.[9,18–20]

As a basis for our experiment we make a simple qualitative prediction on the blinking properties of fluorophores from one homologous series. The absorption properties of cyanines can be described well by Kuhn's free-electron gas model.[17] The model also allows estimating redox potentials assuming that certain energy contributions such as the solvation energy do not change within the homologous series. In this case the LUMO energy is related to the redox potential by Equation (1):

$$-E_{red} = \frac{A}{F} + k \approx -\frac{E_{LUMO}}{F} + k \qquad (1)$$

where A is the electron affinity, F is Faraday's constant and k is a constant that includes the free energy change for solvation.[21] Since the LUMO energy decreases with increasing size of the box, the reduction potential increases. That is, larger fluorophores within a homologous series are reduced more easily. Since the reaction rates of non-diffusion-limited processes are linked to the Gibbs free energy of the reaction, we expect that the re-oxidation of the radical anion will be faster in the order Cy7 > Cy5 > Cy3 under otherwise identical experimental conditions.[22] This means that the OFF-state lifetime of the radical anion should increase in the order Cy3 < Cy5 < Cy7 in a reducing buffer and low concentrations of oxidant. We used molecular oxygen and 1,1′-dimethyl-4,4′-bipyridinium dichloride hydrate (methylviologen, MV) as oxidants.

To study the OFF-state lifetime of the homologous series of cyanines, fluorophores bound to biotinylated DNA were immobilized with BSA-biotin/neutravidin on glass cover slips. For excitation of the fluorophores from different spectral regions, we used a multi-colour single-molecule setup equipped with a supercontinuum laser and acousto-optical components for free wavelength selection. The detection is carried out by avalanche photodiodes and the spectral windows are selected using dichroic mirrors and appropriate filters. For details of the setup see the Experimental Section and refs. [23,24]. After recording

fluorescence images (Figure 2A), fluorescence intensity transients were recorded and analysed using custom-made LabVIEW code and OFF-times were determined by autocorrelation analysis as described in ref. [4]. For the analysis only transients that showed a distinct single bleaching step at the end were selected, which allows for individual background correction. A section of an exemplary transient is depicted in Figure 2B together with the corresponding autocorrelation function (Figure 2C). Besides the component for redox blinking ($\tau_{OFF2}=41$ ms and $\tau_{ON2}=3.8$ ms), a short bunching term ($\tau_{OFF1}=180$ μs and $\tau_{ON1}=20$ μs) is visible that is assigned to *cis–trans* isomerisation common to cyanine dyes.[25] At the conditions used, the average ON- and OFF-times of *cis–trans* isomerisation are τ_{OFF1} (Cy3) = 37 μs and τ_{ON1} (Cy3) = 47 μs, τ_{OFF1} (Cy5) = 165 μs and τ_{ON1} (Cy5) = 22 μs, and τ_{OFF1} (Cy7) = 227 μs and τ_{ON1} (Cy7) = 34 μs for the different dyes, respectively.

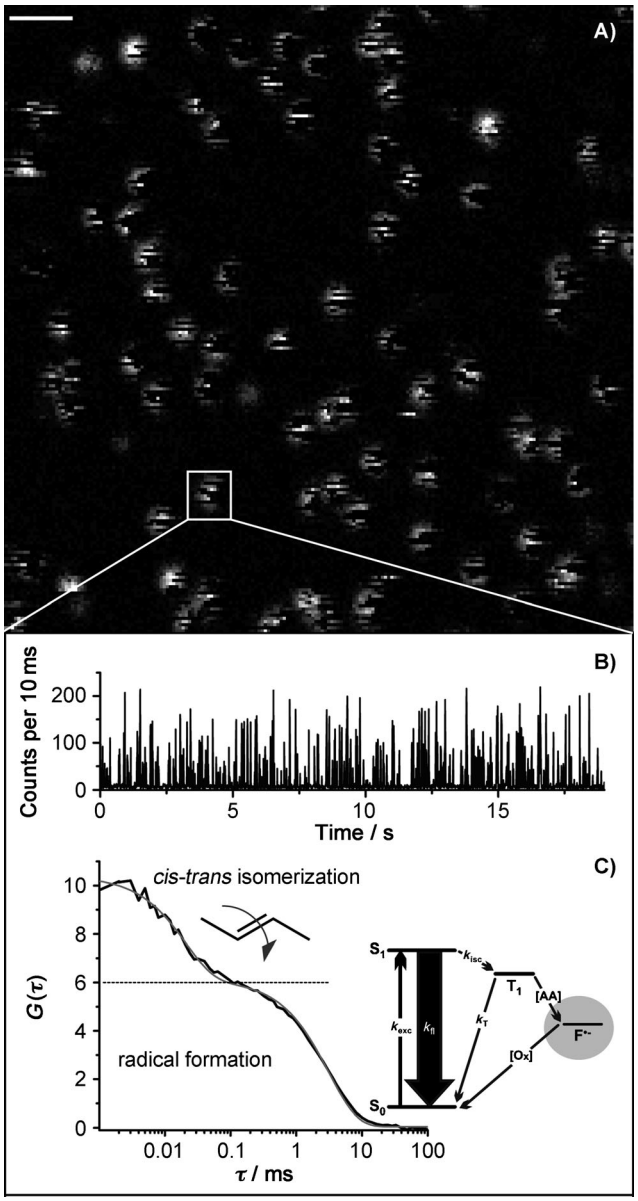

Figure 2. A) Confocal fluorescence intensity image showing immobilized dsDNA-Cy5 molecules in aqueous PBS buffer at pH 7.4. The shown area (10×10 μm, 2 ms/pixel) was scanned by excitation at 640 nm with an average intensity of 3 μW. The scale bar at upper left is 1 μm. Single-molecule blinking due to oxygen removal and the presence of AA ([AA] = 75 μM) is observed as dark pixels in single point spread functions. B) Fluorescence intensity transient recorded under identical experimental conditions. C) Autocorrelation function and biexponential fit of the fluorescent transient shown in (B). The short component, assigned to *cis–trans* isomerization has an OFF-time of $\tau_{OFF}=180$ μs and an ON-time of $\tau_{ON}=20$ μs while the long component, which is assigned to the formation of a radical anion, has an OFF-time of $\tau_{OFF}=41$ ms and an ON-time of $\tau_{ON}=3.8$ ms.

3. Influence of Oxygen on Single-Molecule Blinking

The concentration of the reductant ascorbic acid is chosen to maximize the OFF-state lifetime and is much higher than the oxidant concentration.[10] In the presence of oxygen at atmospheric pressure corresponding to ~500 μM dissolved oxygen, no blinking of Cy5 is observed because triplet as well as radical anionic states are rapidly depleted by reactions with oxygen. Additionally, the molecules bleach quickly due to the formation of singlet oxygen. To also exclude initial photoinduced oxidation by the oxidant we used a significantly lower oxidant than reductant concentration. We can thus safely assume that all observed dark states that cannot be assigned to *cis–trans* isomerisation but represent radical anionic states (with respect to an assumed neutral ground state chromophore). The assumption is justified for two reasons. First, due the concentration difference, reduction from an excited state is more likely than the oxidation. Second, the oxidized state would be too short-lived to be detected at the AA concentration used.

When using oxygen as oxidant, its concentration has to be controlled in a reproducible fashion. To this end, we developed a protocol for oxygen removal by the GOC system that we calibrated with the aid of an oxygen meter. The GOC system allows the removal of dissolved oxygen down to an equilibrium concentration of ~10 μM.[26] To check the oxygen concentration in the single-molecule experiments and to ensure that equilibrium is achieved, we studied the oxygen concentration as a function of time for different glucose oxidase concentrations by monitoring the blinking kinetics of the cyanines. Figures 3A,C show the progression of the OFF-times of Cy5 for two concentrations of glucose oxidase starting directly after addition of GOC and sealing of the chamber (1% v/v vs 10% v/v, see the Experimental Section for details). Each data point represents the average OFF-time obtained for the transient of a single cyanine molecule. The data shown in Figure 3A represent ~400 molecules and Figure 3C ~200 molecules. Both graphs exhibit an initial increase in the OFF-times. Saturation, however, occurs much faster for the higher glucose oxidase concentration after about 10 min whereas saturation is reached after more than 90 min for 1% v/v. In addition, at a lower concentration of the enzyme (1% v/v,) a higher oxygen concentration is indicated by lower mean OFF-times for 1% v/v (12 ± 10 ms) compared to 10% v/v (41 ± 20 ms). Figures 3B,D show the corresponding OFF-time histograms derived after saturation was reached. These results show the importance of a sufficient concentration of glucose oxidase to reach the highest possible OFF-time and also the need to wait for

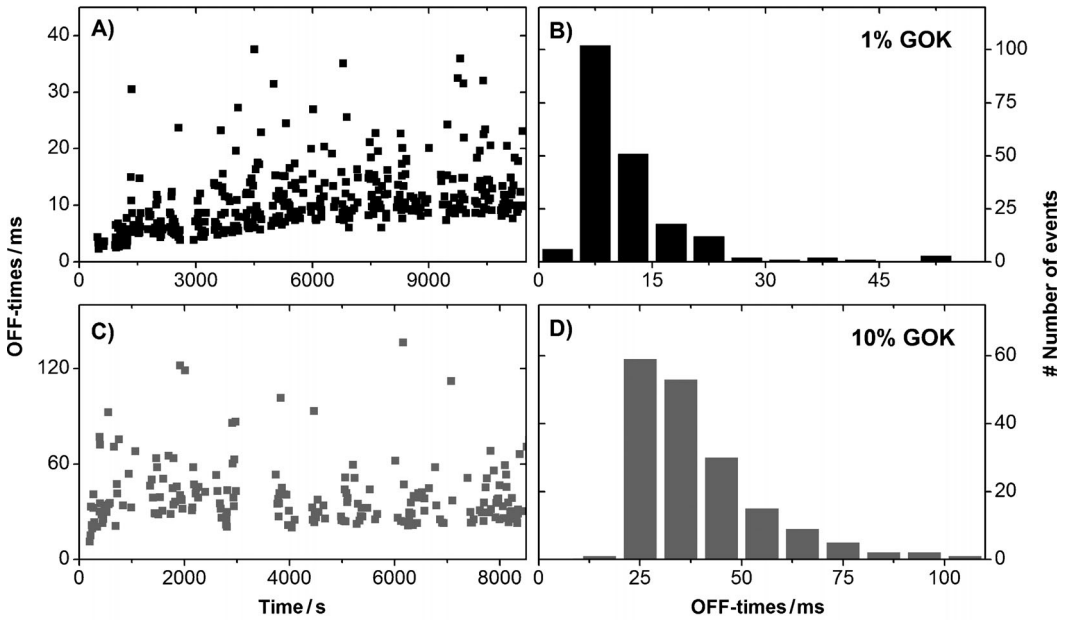

Figure 3. Single-molecule analysis of the OFF-time distribution of immobilized Cy5 molecules at two different concentrations of GOC: A) and C) show the temporal development of the OFF-times after addition of 1% or 10% GOC and sealing of the chamber ($t=0$). The steady state of OFF-times is reached at around $t=6000$ s for 1% GOC and around $t=500$ s for 10% GOC. B) and D) show histograms of the OFF-time distribution after the steady state is reached. The mean value of the distribution is 12 ± 10 ms for 1% GOC and 41 ± 20 ms for 10% GOC.

the system to reach equilibrium. As a consequence we used 10% v/v glucose oxidase for reaching the steady state quickly and reproducibly in all subsequent experiments.

A more subtle detail of the plots in Figures 3 A,C is the asymmetric shape of the distribution. Initially, the OFF-times are quite homogenous and short. With decreasing oxygen concentration the distribution of OFF-times broadens with a remarkably sharp edge for shorter OFF-times. This distribution might reflect sample inhomogeneity with some fluorophores being more exposed to the solution (short OFF-times) and other being better shielded from oxygen by the BSA coating of the surface. A small fraction of individual fluorophore time transients showed switching between distinct OFF-times, which could be an indication of a discrete rearrangement of one fluorophore's specific nano-environment. Moreover, measurements of dsDNA structures with Cy5 at the 5′-end yielded ~50% longer OFF-times for comparable experimental conditions (data not shown, see ref. [10]), indicating the environmental sensitivity of OFF-state lifetimes.

4. Blinking in the Homologous Series Cy3/Cy5/Cy7

The dyes of the homologous series Cy3/Cy5/Cy7 exhibit an increase in chromophore size and number of π electrons that goes along with systematic changes of their spectroscopic and electrochemical properties. Some of these properties are listed in Table 1.

Investigating more than 100 single-molecule transients for each dye reveals a mean OFF-time of 18 ± 8 ms for Cy3 (Figure 4 A), 41 ± 20 ms for Cy5 (Figure 4 B) and 71 ± 23 ms for Cy7 (Figure 4 C). We ascribe the broad distributions to the mentioned variation of the molecules nano-environment, causing a shoulder in the histograms displayed in Figure 4. Nevertheless, the average values of the OFF-time distributions are reproducible within several milliseconds when repeating the experiment, including new surface preparation, immobilization of dye molecules and oxygen removal. Table 1 shows the average OFF-time for multiple repeats ($n\geq3$) consisting of at least 100 evaluated transients per experiment. We also studied the excitation intensity dependence and found that OFF-times slightly decrease for higher excitation powers.[35] For the given conditions, Cy5, for example, exhibits ~25% shorter OFF-times at 5-fold higher excitation intensity. To reduce the influence of sample heterogeneity in addition to calculating the mean values of the distributions we investigated the behaviour of the mentioned sharp edge for shorter OFF-times for the different cyanine dyes. As a quantitative measure for this lower bound we calculated the lowest decile for the distributions and obtained τ_{OFF} (Cy3) = 11 ms, τ_{OFF} (Cy5) = 23 ms, and τ_{OFF} (Cy7) = 52 ms, which additionally confirms the expected trend of OFF-times.

Table 1. Spectroscopic and electrochemical properties of cyanine dyes.[a]

	Cy3	Cy5	Cy7
Abs. (max)	550 nm	649 nm	752 nm
Fl. (max)	570 nm	670 nm	778 nm
E_{red} vs SCE	−1.0 V[28]	−0.84 V[29]	−0.72 V*
τ_{OFF}	18 ms	47 ms	67 ms

[a] *E_{red} for Cy7 was estimated by linear extrapolation of the values for Cy3 and Cy5 according to the absorption energy.[27]

The data allow an estimation of the rate constants of these electron transfer reactions using $\tau_{off}^{-1}=k_{on}=k_{ox}$ [Ox], that is,

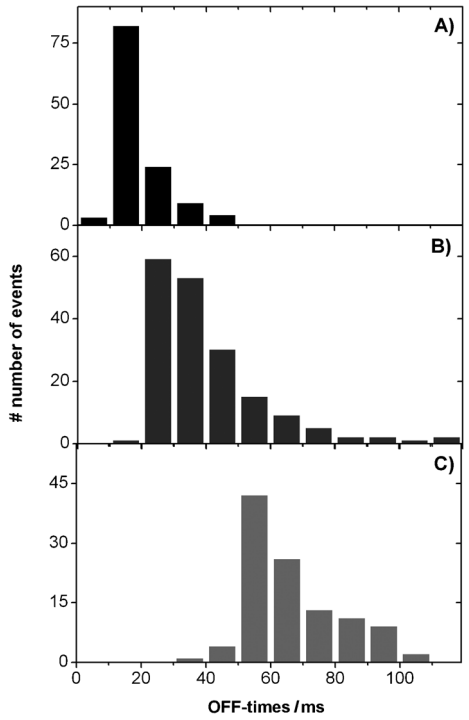

Figure 4. OFF-time histograms of immobilized cyanine molecules at 10% GOC with fully equilibrated oxygen removal. Only time transients showing a single bleaching step at the end are selected. A) Cy3 with a mean value of 18 ± 8 ms, B) Cy5 with a mean value of 41 ± 20 ms, C) Cy7 with a mean value of 71 ± 23 ms.

the rate constant for switching the molecule back ON by the electron transfer to the oxidant k_{ox}. Assuming an oxygen concentration of 10 μM, we obtain k_{ox} in the range of (10^6–10^7) $s^{-1}\,M^{-1}$ for the three dyes. The driving force for the reaction is estimated by the reduction potentials of the fluorophores and the reduction potential of oxygen.[29] The Gibbs energy is $\Delta G = -0.60$ eV for Cy3, $\Delta G = -0.44$ eV for Cy5, and $\Delta G = -0.32$ eV for Cy7, assuming a redox potential of E_{red} (O_2) = −0.40 V vs SCE for 1 mol L^{-1} oxygen concentration.[30] Comparing to typical Rehm–Weller plots,[22,31] the expected order of magnitude for the rate constant of these Gibbs energies is between (10^9–10^{10}) $s^{-1}\,M^{-1}$, that is, several orders of magnitude larger than the observed values. While our data qualitatively meet expectation, we cannot explain the large deviation with respect to the absolute expected values. Possibly, the oxygen concentration is much lower than the measured ~10 μM because this concentration is close to the detection limit of the employed oxygen meter. Additionally, the large increase in OFF-times for many fluorophores from < 1 μs in the presence of oxygen to > 30 ms after enzymatic oxygen removal, that is, by a factor of 3×10^4 can hardly be explained by an oxygen reduction of only 50-fold from 500 μM to 10 μM (see for example refs. [4,29]).

To test whether an overestimation of the oxygen concentration can be the reason for the deviations or whether there might be a more fundamental problem with our model, we used methylviologen (MV) as an alternative oxidant whose concentration is better controlled. We measured the OFF-times of the three dyes at various concentration of MV keeping the AA concentration constant at 75 μM. Oxygen was removed as in previous experiments. For all dyes, the OFF-time already decreases at nanomolar concentrations although MV (E_{red} = 0.69 V vs SCE) has less oxidative potential than oxygen (Figure 5). At

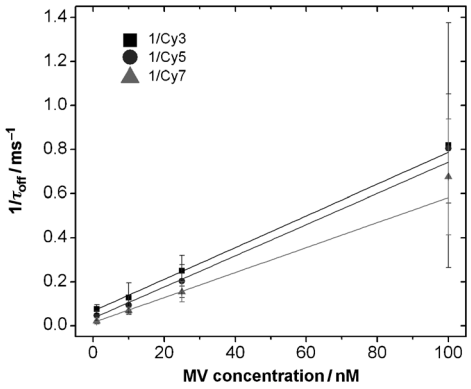

Figure 5. Plot of the dependence of the inverse OFF-times on MV concentration for Cy3 (■), Cy5 (●) and Cy7 (▲). Fits are according to Equation (2): k_{ox} (Cy7) = 5.68×10^9 $s^{-1}\,M^{-1}$, k_{ox} (Cy5) = 7.08×10^9 $s^{-1}\,M^{-1}$, and k_{ox} (Cy3) = 7.20×10^9 $s^{-1}\,M^{-1}$.

concentrations greater than 100 nM the OFF-times become so short that they cannot clearly be distinguished from blinking due to *cis–trans* isomerisation. To determine the rate constants for this system, we fitted the data in Figure 5 by Equation (2):

$$1/\tau_{off} = k_{ox}[MV] + k'_{ox}[O_2] = k_{ox}[MV] + \text{constant} \quad (2)$$

The offset in the equation accounts for the fact that the remaining oxygen concentration also contributes to the shortening of the OFF-state lifetime, that is, the OFF-state lifetime is not infinite in the absence of MV. The fits yield the reaction rate constants k_{ox} (Cy7) = 5.68×10^9 $s^{-1}\,M^{-1}$, k_{ox} (Cy5) = 7.08×10^9 $s^{-1}\,M^{-1}$, and k_{ox} (Cy3) = 7.20×10^9 $s^{-1}\,M^{-1}$. Taking into account a Gibbs energy for the reaction with MV (E_{red} = 0.69 V vs SCE) of $\Delta G = -0.31$ eV for Cy3, $\Delta G = -0.15$ eV for Cy5, and $\Delta G = -0.03$ eV for Cy7, these values match expectations from Rehm–Weller plots very well.[22] The stronger driving forces for Cy5 and Cy3 yield similar values for their quenching constant since the values approach the diffusional plateau. Cy7 only has a small driving force explaining the larger difference between Cy7 and Cy5 compared to Cy5 and Cy3. Considering the small driving force for Cy7 the observed value for k_{ox} is still relatively high. In summary, the kinetics of the oxidation of radical anions by MV corroborates the proposed model and suggests the tight connection between OFF-states of single-molecule redox blinking and chromophores' electronic properties. In addition variations by different local environments of the fluorophores are indicated.

5. Conclusions

We have studied redox blinking of a homologous series of cyanine dyes. The underlying radical anionic states were induced

by removing oxidants (i.e. oxygen) and by adding the reductant ascorbic acid. We found that for different conditions the OFF-state lifetime was increasing in the order Cy3 < Cy5 < Cy7. The behavior was related to the reduction potential of the fluorophores which increases with the size of the chromophore. Thus, we could qualitatively predict blinking properties of fluorophores on the simple basis of the free-electron gas model that a better stabilized radical anion yields longer OFF-state lifetimes. Interestingly, we found reaction rates of the radical anion that were unexpectedly low at the assumed oxygen concentration. On the other hand, reaction rates met the expectations of similar Rehm–Weller plots when methylviologen (MV) was used as oxidant confirming the model of photoinduced reduction and oxidation reactions.[29] The deviation between the results obtained with oxygen and MV as oxidants might be explained by overestimated oxygen concentrations. On the other hand, assuming similar quenching constants for MV and oxygen, oxygen exhibits an activity as if it was present at an effective concentration between 1–10 nM as estimated from the fits in Figure 5. Our data also shed new light on the nature of the underlying dark states in super-resolution microscopy that relies on the successive localization of single molecules. Tetramethylrhodamine (TMR), for example, was used in live-cell super-resolution imaging and exhibited pronounced blinking with long OFF-states.[32,33] TMR has an estimated reduction potential of E_{red} (TMR) = −0.95 V vs SCE,[34] yielding a driving force for the back electron transfer between that of Cy3 and Cy5. From these values, OFF-states long enough for imaging at 50 Hz in living cells are not expected. This either indicates that the nature of the underlying OFF-state might be different. Alternatively, the oxygen activity might be reduced or oxygen is heavily consumed due to the irradiation in the presence of thiols.[15]

Experimental Section

Sample Preparation

Samples for single-molecule experiments were prepared based on DNA oligonucleotides. A 40-mer oligonucleotide labelled with a single fluorophore at position 24 (TAC GAT TCG ATT CCT TAC ACT TA*X* ATT GCA TAG CTA TAC G; *X* = T-Cy3/Cy5/Cy7; as received from IBA, Germany compare Figure 1) was hybridized to a biotinylated counter-strand (also from IBA, Germany). All experiments were carried out at room temperature (22 °C) under the following buffer conditions. Standard phosphate-buffered saline (PBS) with a pH of 7.4 was used in combination with enzymatic oxygen removal (PBS, pH 7.4, containing 10% (wt/v) glucose was mixed with either 10% (v/v) or 1% (v/v) of a prior prepared glucose oxidase solution. This solution was prepared according to the following protocol: 40 μL Tris(2-carboxyethyl)phosphine hydrochloride (TCEP), 40 μL catalase and 10 mg glucose oxidase type VIII were added to 5 mL of TRIS buffer [100 mM TRIS(HCl) pH 7.5, 25 mM KCl] and mixed with 5 mL of glycerine (all purchased from Sigma). Additionally, 75 μM of the reductant ascorbic acid (AA) were added. Surface scans and transients were performed in a chambered cover slide (LabTek, NUNC) with a volume of ~750 μL sealed with microseal adhesive seals (MSB 1001, Bio-Rad, Germany).

Calibration of Oxygen Removal

To calibrate the oxygen removal of the GOC system described above we used a dissolved-oxygen meter (OxyScan light, equipped with a micro oxygen sensor for low sample volumes, UMS GmbH, Germany). Due to the size and characteristics of the sensor, higher sample volumes of around 8 mL had to be used and a magnetic stir bar was employed to ensure a constant flow. Sealing of the small beaker glass was also performed with microseal adhesive seals. For measurements with 10% GOC an equilibrium concentration of ~10 μM oxygen was reached after approximately 10 min, which is in good agreement with prior published data under similar conditions.[26]

Single-Molecule Spectroscopy

Double-stranded DNA (dsDNA) was immobilized on a glass substrate coated with BSA/biotin-streptavidin according to published procedures. By homogenizing the environment through immobilization of fluorophores in solution the static heterogeneity of the molecules is greatly reduced and thus allows the extraction of detailed kinetic information through the analysis of single-molecule fluorescence transients. To study fluorescence on the level of single molecules, a custom-built confocal microscope was used as described in refs. [1,23] (detection of Cy3/Cy5: ref. [1], detection of Cy7: ref. [23]). The laser beam of a pulsed supercontinuum source (SuperK Extreme, Koheras, Denmark) was coupled into a single-mode fiber and appropriate excitation light was chosen by an acoustic-optical tunable filter (AOTFnc-VIS, AA optoelectronic). The following excitation wavelengths were chosen: 533 nm (excitation of the Cy3), 640 nm (excitation of Cy5) and 725 nm (excitation of Cy7). The spatially filtered beam entered an inverse microscope and was coupled into an oil immersion objective (60×, NA 1.35, UPLSAPO 60XO, or 100×, NA 1.45, PLAPO100XO/TIRFM-SP, both from Olympus) by a dual-band dichroic beam splitter (Dualband z532/633 rpc for Cy5/Cy7 and a 740 DCXXR for Cy7, AHF Analysentechnik, Germany). Fluorescence transients and confocal images (size of 10 μm × 10 μm, integration time 2 ms per pixel, 50 nm per pixel) were recorded under the following conditions: 1.5 kW cm^{-2} at 533 nm, 3 kW cm^{-2} at 640 nm, and 8 kW cm^{-2} at 725 nm. The resulting fluorescence was collected by the same objective, focused onto a 50 μm pinhole, and split spectrally at 640 nm onto two APDs for Cy3/Cy5 by a dichroic beam splitter (640DCXR, AHF Analysentechnik, Germany) or onto a 120 μm pinhole and directly imaged onto only one APD for Cy7. Fluorescence was detected by avalanche photodiodes (SPCM-AQR-14, PerkinElmer) with appropriate spectral filtering (Brightline HC582/75 for Cy3, ET-Bandpass 700/75 M and Razoredge longpass for Cy5, Brightline HC 785/62 for Cy7, AHF Analysentechnik, Germany).

Data Evaluation and Analysis

The detector signal was registered and evaluated using custom made LabVIEW software. Single-molecule traces and autocorrelation analysis was performed according to published procedures.[4]

Acknowledgements

We thank Jan Vogelsang, Frederik Becher, Christian Steinhauer and Andreas Gietl for experimental assistance. I. H. Stein is grateful to the Elite Network of Bavaria (International Doctorate Program in NanoBioTechnology) for a doctoral fellowship. T. Cordes was supported by the Centre of Synthetic Biology (University of

Groningen) and the Center for NanoScience (CeNS, LMU München). P. Tinnefeld was supported by the DFG (Ti329/5-1), Biophotonics IV program of the German Ministry of Research and Education (BMBF/VDI), the Center for NanoScience (CeNS, LMU München) and the excellence cluster Nanosystems Initiative Munich.

Keywords: dyes/pigments · fluorescence spectroscopy · photophysics · single-molecule studies · super-resolution microscopy

[1] J. Vogelsang, T. Cordes, P. Tinnefeld, *Photochem. Photobiol. Sci.* **2009**, *8*, 486 – 496.
[2] M. Orrit, *Photochem. Photobiol. Sci.* **2010**, *9*, 637 – 642.
[3] R. Zondervan, F. Kulzer, S. B. Orlinskii, M. Orrit, *J. Phys. Chem. A* **2003**, *107*, 6770 – 6776.
[4] J. Vogelsang, T. Cordes, C. Forthmann, C. Steinhauer, P. Tinnefeld, *Proc. Natl. Acad. Sci. USA* **2009**, *106*, 8107 – 8112.
[5] S. W. Hell, M. Kroug, *Appl. Phys. B* **1995**, *60*, 495 – 497.
[6] E. Betzig, G. H. Patterson, R. Sougrat, O. W. Lindwasser, S. Olenych, J. S. Bonifacino, M. W. Davidson, J. Lippincott-Schwartz, H. F. Hess, *Science* **2006**, *313*, 1642 – 1645.
[7] M. J. Rust, M. Bates, X. Zhuang, *Nat. Methods* **2006**, *3*, 793 – 795.
[8] S. T. Hess, T. P. Girirajan, M. D. Mason, *Biophys. J.* **2006**, *91*, 4258 – 4272.
[9] M. Heilemann, S. van de Linde, M. Schuttpelz, R. Kasper, B. Seefeldt, A. Mukherjee, P. Tinnefeld, M. Sauer, *Angew. Chem.* **2008**, *120*, 6266 – 6271; *Angew. Chem. Int. Ed.* **2008**, *47*, 6172 – 6176.
[10] C. Steinhauer, C. Forthmann, J. Vogelsang, P. Tinnefeld, *J. Am. Chem. Soc.* **2008**, *130*, 16840 – 16841.
[11] J. Fölling, M. Bossi, H. Bock, R. Medda, C. A. Wurm, B. Hein, S. Jakobs, C. Eggeling, S. W. Hell, *Nat. Methods* **2008**, *5*, 943 – 945.
[12] T. Dertinger, R. Colyer, G. Iyer, S. Weiss, J. Enderlein, *Proc. Natl. Acad. Sci. USA* **2009**, *106*, 22287 – 22292.
[13] J. Vogelsang, C. Steinhauer, C. Forthmann, I. H. Stein, B. Person-Skegro, T. Cordes, P. Tinnefeld, *ChemPhysChem* **2010**, *11*, 2475 – 2490.
[14] T. Cordes, J. Vogelsang, M. Anaya, C. Spagnuolo, A. Gietl, W. Summerer, A. Herrmann, K. Mullen, P. Tinnefeld, *J Am Chem. Soc.* **2010**, *132*, 2404 – 2409.
[15] S. van de Linde, I. Krstic, T. Prisner, S. Doose, M. Heilemann, M. Sauer, *Photochem. Photobiol. Sci.* **2011**, *10*, 499 – 506.
[16] S. van de Linde, R. Kasper, M. Heilemann, M. Sauer, *Appl. Phys. B* **2008**, *93*, 725 – 731.
[17] H. Kuhn, *Helv. Chim. Acta* **1949**, *32*, 2247.
[18] M. Levitus, S. Ranjit, *Q. Rev. Biophys.* **2011**, *44*, 123 – 151.
[19] S. Lee, J. Lee, S. Hohng, *PLoS ONE* **2010**, *5*, e12270.
[20] M. Bates, B. Huang, G. T. Dempsey, X. Zhuang, *Science* **2007**, *317*, 1749 – 1753.
[21] M. J. S. Dewar, J. A. Hashmall, N. Trinajstic, *J. Am. Chem. Soc.* **1970**, *92*, 5555 – 5559.
[22] A. Rosspeintner, D. R. Kattnig, G. Angulo, S. Landgraf, G. Grampp, *Chem. Eur. J.* **2008**, *14*, 6213 – 6221.
[23] I. H. Stein, C. Steinhauer, P. Tinnefeld, *J. Am. Chem. Soc.* **2011**, *133*, 4193 – 4195.
[24] J. Ross, P. Buschkamp, D. Fetting, A. Donnermeyer, C. M. Roth, P. Tinnefeld, *J. Phys. Chem. B* **2007**, *111*, 321 – 326.
[25] J. Widengren, P. Schwille, *J. Phys. Chem. A* **2000**, *104*, 6416 – 6428.
[26] C. E. Aitken, R. A. Marshall, J. D. Puglisi, *Biophys. J.* **2008**, *94*, 1826 – 1835.
[27] E. S. Pysh, N. C. Yang, *J. Am. Chem. Soc.* **1963**, *85*, 2124 – 2130.
[28] J. Lenhard, *J. Imaging Sci.* **1986**, *30*, 27 – 35.
[29] J. Vogelsang, R. Kasper, C. Steinhauer, B. Person, M. Heilemann, M. Sauer, P. Tinnefeld, *Angew. Chem.* **2008**, *120*, 5545 – 5550; *Angew. Chem. Int. Ed.* **2008**, *47*, 5465 – 5469.
[30] P. M. Wood, *Biochem. J.* **1988**, *253*, 287 – 289.
[31] D. Rehm, A. Weller, *Isr. J. Chem.* **1970**, *8*, 259 – 271.
[32] I. Testa, C. A. Wurm, R. Medda, E. Rothermel, C. von Middendorf, J. Folling, S. Jakobs, A. Schonle, S. W. Hell, C. Eggeling, *Biophys. J.* **2010**, *99*, 2686 – 2694.
[33] T. Klein, A. Loschberger, S. Proppert, S. Wolter, S. van de Linde, M. Sauer, *Nat. Methods* **2011**, *8*, 7 – 9.
[34] J. R. Unruh, G. Gokulrangan, G. S. Wilson, C. K. Johnson, *Photochem. Photobiol.* **2005**, *81*, 682 – 690.
[35] P. Tinnefeld, V. Buschmann, K. D. Weston, M. Sauer *J. Phys. Chem. A* **2003**, *107*, 323 – 327.

Received: October 16, 2011
Published online on December 8, 2011

